ChemComm

Accepted Manuscript

This article can be cited before page numbers have been issued, to do this please use: F. Xu, Y. Zhu, Z. Ma, W. Zhao, J. Xu and H. Chen, *Chem. Commun.*, 2016, DOI: 10.1039/C5CC09963C.

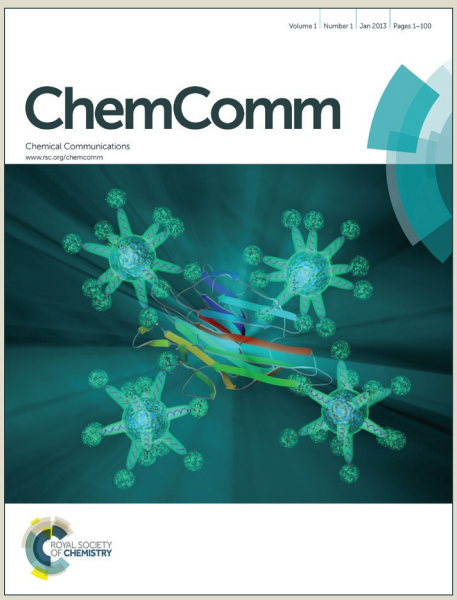

ROYAL SOCIETY OF CHEMISTRY

www.rsc.org/chemcomm

ChemComm

View Article Online
DOI: 10.1039/C5CC09963C

COMMUNICATION

An Ultrasensitive Energy-transfer Based Photoelectrochemical Protein Biosensor

Received 00th January 20xx,
Accepted 00th January 20xx

DOI: 10.1039/x0xx00000x

www.rsc.org/

Fei Xu†, Yuan-Cheng Zhu†, Zheng-Yuan Ma, Wei-Wei Zhao*, Jing-Juan Xu* and Hong-Yuan Chen

Using single stranded DNA (ssDNA) as a distance controller and Au nanoparticles (NPs) functionalized with ssDNA as novel energy-transfer nanoprobes, an ultrasensitive energy-transfer based photoelectrochemical protein biosensor was realized.

The development of novel biosensors for highly sensitive, rapid, and specific protein detection is of significant importance for disease diagnosis, medicine research, food safety and environmental monitoring.[1,2] Recent have witnessed tremendous advances towards using various optical, electrochemical and photoelectrochemical systems[3-19] for specific protein detections and many exquisite signaling mechanisms, such as various resonance energy transfer processes (including fluorescence, bioluminescence, chemiluminescence, electrochemiluminescent, etc.),[20-23] have been extensively studied. In this communication, we report for an ultrasensitive protein detection based on the gold nanoparticles (Au NPs) functionalized with nucleic acid strand as novel energy-transfer nanoprobes in a properly designed photoelectrochemical system. We apply the nucleic acid as a facile mediator with tagged Au NPs to stimulate the exciton−plasmon interactions (EPI) for protein detection. It occurs with high sensitivity and selectivity by photocurrent quenching of CdS quantum dots (QDs) induced by EPI between Au NPs nanoprobes and CdS QDs on the electrode.

The energy-transfer based system for protein detection is formulated in Scheme 1. Exciton and plasmon are two most typical excited states of nanomaterials, and the EPI represents a fundamental light-matter interplay that has earlier been demonstrated as a unique phenomenon for biodetection.[24-26] However, to date the highly sensitive protein assay using this unique phenomenon has still been difficult due to various reasons. In the present model system, the anti-thrombin G-quadruplex sequence are immobilized on the CdS QDs modified indium tin oxide (ITO) electrode (Fig. S1 and S2 in the ESI†) by the carbodiimide-assisted amidation reaction and the thrombin is captured and then sandwiched by another G-quadruplex aptamer tagged with Au NPs. The clamp of thrombin is verified by observing the photocurrent quenching of CdS QDs by interparticle EPI. To achieve such detection, we first prepared the Au NP-linked G-quadruplex aptamer which contains a section of single stranded DNA molecules. We verify the successful preparation of Au NP-aptamer nanoprobes by UV-Vis absorbance spectra. As shown in Fig. 1A, comparing with the characteristic absorbance peak of Au NPs (at ca. 520 nm) and nucleic acid aptamer (at ca. 260 nm), the absorbance spectrum of Au-aptamer retained both the two slightly red-shifted peaks, indicating that aptamer had linked to Au NP. Modulation of the single stranded DNA length can serve as a facile distance controller and thus place the Au NPs in proximity of CdS QDs, which can resolve difficulties in the implementation of EPI in common electrochemical or optical protein detections such as the comparatively large sizes or insulating features of protein molecules. After a series of optimization, we selected the nanoprobes which contain 65-mer single stranded DNA molecules for following detection. X-ray photoelectron spectroscopy (XPS), as shown in Fig. 1B, certified presence of Au, C and N in the synthesized bioconjugate. The appearance of a shoulder around 400 eV could be attributed to the nitrogen element came from the aptamer after the conjugation, also suggesting the preparation of Au NP-aptamer nanoprobes.

The efficient excitation of EPI requires a sufficient spectra overlap between the exciton band and the plasmon band. The typical absorption spectrum of the CdS QDs and Au NPs were recorded, respectively (Fig. S3 in the ESI†). The absorption spectrum implies that the CdS QDs have a broad absorption range that is suitable for employment as photoactive substrate. Besides, CdS QDs have an emission peak at around 510 nm. Meanwhile, the absorption spectrum of the Au NPs is clearly characterized by the symmetrical plasmon peak of Au NPs at around 520 nm. The excitonic emission of the CdS QDs has a large spectral overlap with the plasmon absorption of the Au NPs, which would be beneficial to the inducement of the plasmon of Au NPs and thus the generation of EPI. Besides, when in near close, Au NPs would also introduce a

[a] State Key Laboratory of Analytical Chemistry for Life Science and Collaborative Innovation Center of Chemistry for Life Sciences, Nanjing University, Nanjing 210023, China. E-mail: zww@nju.edu.cn xujj@nju.edu.cn

† These authors contribute to this work equally.

Electronic Supplementary Information (ESI) available: Materials, methods and supplementary data. See DOI: 10.1039/x0xx00000x

non-radiative decay route in CdS QDs. The insets in Fig. S3 A and B are the TEM images of the CdS QDs and Au NPs, respectively.

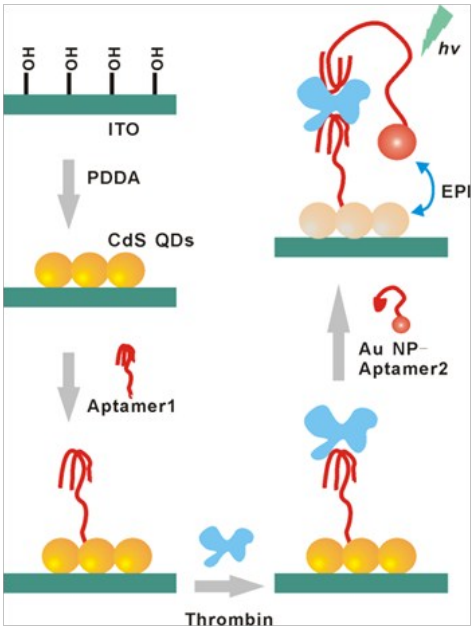

Scheme 1. Schematic mechanism of the operating biosensor system.

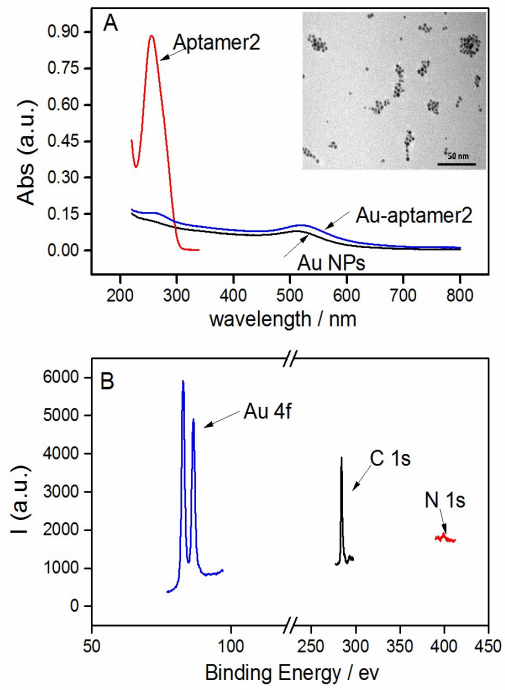

Fig. 1 A) UV-Vis absorption spectrum of Au NPs, bare aptamer2 and Au-aptamer2, the inset is TEM of Au-aptamer2. B) The XPS spectrum of Au-aptamer2.

Intermittent visible light irradiation was applied to acquire the transient photocurrent responses for each step during the biosensor development. Fig. 2 records the corresponding photocurrent changes under the monochromatic irradiation of 410 nm light. After anchoring aptamer1 and blocking by monoethanolamine, the photocurrent decrease about 21% as compared to the initial intensity, which can be discerned from curves a, b and c respectively. This decrease should be attributed to the enhanced steric hindrance of the electrode surface that impeded the diffusion of electron donor to the CdS QDs surface. After the thrombin was captured on the electrode by the specific binding between the thrombin and aptamer, photocurrent intensity further decreased with as shown by curve d. When the Au NPs and CdS QDs in close proximity, the radiative decay in CdS QDs along with the spontaneous emission would stimulate the plasmon resonance of the proximal Au NPs and thereby generate local electric fields that in turn modulate the exciton states in the CdS QDs by enhancing the radiative decay rate, which would compete with the electron transfer from the CdS QDs to the ITO electrode. After the Au-aptamer2 was fixed on the captured protein, an obvious decrease of around 50% photocurrent intensity could be observed. In fact, Au NPs would meanwhile create a non-radiative decay route for electron-hole recombination in CdS QDs with exciton energy transfer from the CdS QDs to the Au NPs, the factor of which also contributed to the photocurrent quenching of CdS QDs.[24-26] In Fig. 3，we compared the Au-aptamer2 nanoprobes to the bare aptamer2, and the current reduction of Au-aptamer2 was obviously greater than the bare aptamer2.

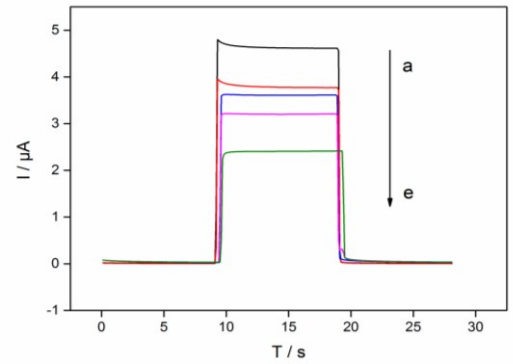

Fig. 2 Photocurrent intensity in 0.10 M PBS containing 0.10 M ascorbic acid of (a) PDDA/CdS modified ITO electrode, (b) modified with 25 μL, 1 μM aptamer1 and (c) blocked by MEA, (d) combined with thrombin, (e) linked with Au NPs-labeled aptamer2. The concentration of thrombin was 1.0×10^{-11} M. The working potential was 0.0 V and the excitation wavelength was 410 nm.

A limit-of-detection study was performed by varying the concentration of thrombin from 1.0×10^{-16} M to 1.0×10^{-10} M. As shown in Fig. 4, the ΔI was reduced in proportion to the decreased protein concentration, reflecting that with increased the protein concentration, more Au-aptamer2 nanoprobes would be confined to the electrode surface. Thus the photocurrent decreased greatly resulting from the effect of interparticle energy transfer. The photocurrent decrease, as shown in the Fig. 4 inset, was with the linear range from 1.0×10^{-15} M to 1.0×10^{-11} M (R^2=0.997) with the a detection limit of 1.0×10^{-16} M, and the detection limit was much lower than recently reported detection of thrombin,[27-29] indicating the superiority of this novel energy-transfer based protein biosensor.

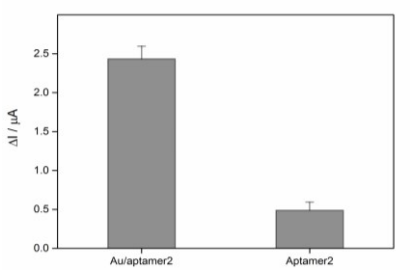

Fig. 3 Effect of different modification on the differential photocurrent responses ($\Delta I = I_0 - I$, I_0 is the photocurrents of MEA/aptamer1/CdS/ITO electrode, and I is the photocurrents of Au-aptamer2 or aptamer2 /thrombin/ MEA/aptamer1/CdS/ITO.

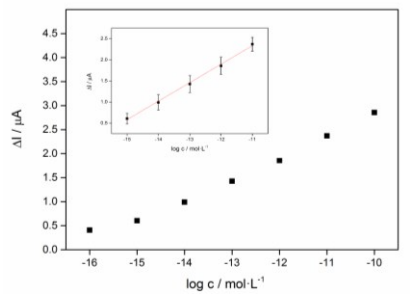

Fig. 4 Effect of different concentrations of thrombin on the differential photocurrent responses ($\Delta I = I_0 - I$, I_0 is the photocurrents of MEA/aptamer1/CdS/ITO electrode, and I is the photocurrents of Au/aptamer2/thrombin/MEA/aptamer1/CdS/ITO. Insert: the corresponding calibration curve. The photocurrent measurement was carried out in 0.10 M PBS containing 0.10 M AA. The working potential was 0.0 V and the light wavelength was 410 nm.

To study the selectivity of the biosensor, we used different protein for incubation with same concentration (1.0×10^{-9} M) following the same procedure, and then compared the resulting photocurrent decrease with the thrombin (1.0×10^{-13} M), Fig. 5. The unmatched proteins could not cause Au-aptamer2 immobilization and thus no obvious photocurrent reduction. In the case of the thrombin, however, a significant decrease was observed, revealing the specificity of its aptamers towards thrombin. Incidentally, because lysozyme is the electropositive under normal physiological pH condition, it could interact with the negatively charged DNA non-specifically. High concentration of lysozyme was more easily to disturb the thrombin detection.

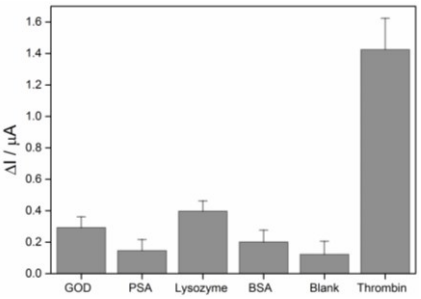

Fig. 5 The selectivity of electrode toward different analytes, the concentrations of BSA, Lysozyme, GOD, PSA were 1.0×10^{-9} M, the concentration of Thrombin was 1.0×10^{-13} M.

In conclusion, this study introduces an ultrasensitive energy-transfer based protein biosensor. Using single stranded DNA as a unique distance controller and Au NPs-single stranded DNA as novel energy-transfer nanoprobes, the model protein of thrombin could be detected down to the level of 10^{-16} M, which is comparable to other reported analysis methods. These results not only opened a different horizon for future construction of the energy transfer system between various QDs and noble metal NPs, but also offered a feasible mechanism for new ultrasensitive protein detection through a judiciously designed nanosystem. More significantly, since numerous common sandwich immunoassays could also be integrated into the present protocol, this work could be extended as a general sensing basis for those proteins.

View Article Online
DOI: 10.1039/C5CC09636

We acknowledge the financial support from the 973 Program (Grant 2012CB932600), the National Natural Science Foundation of China (Grant Nos.21327902, 21135003 and 21305063), the Natural Science Funds of Jiangsu Province (Grant BK20130553), the Fundamental Research Funds for the Central Universities (Grant 20620140748), and the State Key Laboratory of Analytical Chemistry for Life Science (5431ZZXM1503) for support. This work was also supported by a Project Funded by the Priority Academic Program Development of Jiangsu Higher Education Institutions.

Notes and references

1 J. P. Couturier, M. Sütterlin, A. Laschewsky, C. Hettrich and E. Wischerhoff, *Angew. Chem. Int. Ed.,* 2015, **54**, 6641-6644.
2 N. A. W. Bell and U. F. Keyser, *J. Am. Chem. Soc.*, 2015, **137**, 2035-2041.
3 W. W. Zhao, J. J. Xu and H. Y. Chen, *Chem. Soc. Rev.*, 2015, **44**, 729-741.
4 N. Sabir, N. Khan, J. Völkner, F. Widdascheck, P. del Pino, G. Witte, M. Riedel, F. Lisdat, M. Konrad and W. J. Parak, *Small.*, 2015, DOI: 10.1002/smll.201501883.
5 J. Tang, Y. Y. Zhang, B. Kong, Y. C. Wang, P. M. Da, J. Li, A. Elzatahry, D. Y. Zhao, X. G. Gong and G. F. Zheng, *Nano Lett.*, 2014, **14**, 2702-2708.
6 R. Freeman, J. Girsh and I. Willner, *ACS Appl. Mater. Interfaces.*, 2013, **5**, 2815-2834.
7 W. W. Zhao, J. J. Xu and H. Y. Chen, *Chem. Rev.*, 2014, **114**,7421-7441.
8 W. W. Zhao, X. Y. Dong, J. Wang, F. Y. Kong, J. J. Xu and H. Y. Chen, *Chem. Commun.*, 2012, **48**, 5253-5255.
9 F. Haddache, A. Le Goff, B. Reuillard, K. Gorgy, C. Gondran, N. Spinelli, E. Defrancq and S. Cosnier, *Chem. Eur. J.*, 2014, **20**, 15555-15560.
10 H. Zhou, J. Liu and S. S. Zhang, *TrAC, Trends Anal. Chem.*, 2015, **67**, 56-73.
11 W. W. Zhao, S. Shan, Z. Y. Ma, L. N Wan, J. J. Xu and H. Y. Chen, *Anal. Chem.*, 2013, **85**, 11686-11690.
12 A. Devadoss, P. Sudhagar, C. Terashima, K. Nakata and A. Fujishima, *J. Photochem. Photobiol. C.*, 2015, **24**, 43-63.
13 Y. P. Wu, B. T. Zhang and L. H. Guo, *Anal. Chem.*, 2013, **85**, 6908-6914.
14 W. W. Zhao, L. Zhang, J. J. Xu and H. Y. Chen, *Chem. Commun.*, 2012, **48**, 9456-9458.
15 D. Chen, H. B. Feng and J. H. Li, *Chem. Rev*, 2012, **112**, 6027-6503.
16 W. W. Zhao, J. Wang, J. J. Xu and H. Y. Chen, *Chem. Commun.*, 2011, **47**, 10990-10992.
17 Y. T. Long, C. Kong, D. W. Li, Y. Li , S. Chowdhury and H. Tian, *Small.*, 2011, **7**, 1624-1628.

View Article Online
DOI: 10.1039/C5CC09963C

18 G. L. Wang, J. X. Shu, Y. M. Dong, X. M. Wu, W. W. Zhao, J. J. Xu and H. Y. Chen, *Anal. Chem.*, 2015, **87**, 2892-2900.
19 A. J. Boersma, I. S. Zuhorn and B. Poolman, *Nat. Methods.*, 2015, **12**, 227-229.
20 L. A. Stoddart, E. K. M. Johnstone, A. J. Wheal, J. Goulding, M. B. Robers, T. Machleidt, K. V. Wood, S. J. Hill and K. D. G. Pfleger, *Nat. Method.*, 2015, **12**, 661-663.
21 Y. Xiao, L. Y. Zeng, T. Xia, Z. J. Wu and Z. H. Liu, *Angew. Chem. Int. Ed.*, 2015, **54**, 5323-5327.
22 W. W. Zhao, C. Y. Tian, J. J. Xu and H. Y. Chen, *Chem. Commun.*, 2012, **48**, 895-897.
23 C. M. Lemon, E. Karnas, X. X. Han, O. T. Bruns, T. J. Kempa, D. Fukumura, M. G. Bawendi, R. K. Jain, D. G. Duda and D. G. Nocera, *J. Am. Chem. Soc.*, 2015, **137**, 9832-9842.
24 J. Lee, P. Hernandez, J. Lee, A. O. Govorov and N. A. Kotov, *Nat. Mater.*, 2007, **6**, 291-295.
25 Z. H. Nie, A. Petukhova and E. Kumacheva, *Nature Nanotech.*, 2010, **5**, 15-25.
26 W. W. Zhao, P. P. Yu, Y. Shan, J. Wang, J. J. Xu and H. Y. Chen, *Anal. Chem.*, 2012, **84**, 5892-5897.
27 W. J. Yao, A. L. Goff, N. Spinelli, M. Holzinger, G. W. Diao, D. Shan, E. Defrancq and S. Cosnier, *Biosensors and Bioelectronics.*, 2013, **42**, 556-562.
28 S. G. Li, W. Zhu, Y. C. Xue and S. Q. Liu, *Biosensors and Bioelectronics.*, 2015, **64**, 611-617.
29 X. R. Zhang, Y. P. Xu, Y. Q. Yang, X. Jin, S. J. Ye, S. S. Zhang and L. L. Jiang, *Chem. Eur. J.*, 2012, **18**, 16411-16418.